HELICOPTER TAIL ROTOR STALL FLUTTER

Mikhail Rozhdestvensky

Mil Moscow Helicopter Plant, USSR

Abstract

Stall flutter occurring on helicopter tail rotor blades in hovering and showing an abrupt growth in the value of the pitching moment variable component is investigated in the paper. The values of the measured loads exceed the ordinary level encountered in operation by several times.

The analytical and theoretical investigation of stall flutter has been carried out on a basis of unsteady aerodyanmics, using a model of the blade elastic in bending and torsion. The mechanism of the evolution of self-oscillations and the influence of various design parameters have been investigated. Good qualitative and quantitative agreement of analytical and experimental data has been obtained; means to reduce the pitching moment have been found. Full-scale tests of the Mi-26 tail rotor have confirmed the efficiency of the implemented design solutions aimed at eliminating stall flutter.

Introduction

The improvement of the helicopter weight efficiency, the increase in the service lives of the helicopter main components are inseparably connected with a variety of dynamic and aeroelastic problems to be solved. The problems associated with dynamic strength are essential in ensuring the strength of the helicopter components, the tail rotor in particular. The possibility of designing rotors possessing a permissible level of variable stresses in their blades, hub and control members is defined by the optimal dynamic characteristics obtainable through a rational distribution of the natural frequencies relative to those of the external loads, as well as through the absence of self-oscillations of flexural-torsional and stall flutter types.

The problem of stall flutter has drawn attention due to the growth of the helicopter airspeeds, payload capacity and weight efficiency. Unlike the main rotor in which stall flutter takes place at high airspeeds, tail rotor flutter occurs in hovering and during hovering turns because the tail rotor blades have the

highest angles of attack under these conditions. The increase in the payload capacity with an improvement of the weight efficiency results in higher loading of the helicopter components. For the tail rotor, this means an expansion of the range of the operating blade angles in the part containing maximum values and, respecvely, an increase in the angles of attack approaching the stall ones.

Essential Analytical Techniques

It is typical of stall flutter that the amplitude of the blade torsional vibrations grows limitedly reaching some limit value for each operating condition. However, the overshooting of the pitching moment amplitudes can be so great that the fatigue strength of the tail rotor control cannot be ensured.The Mil Moscow Helicopter Plant experience has shown that some modifications of the tail rotor design could not be put into production due to the occurrence of stall flutter in several cases.

The prediction is based on the solution of differential equations expressing the motion of the blade subject to unsteady aerodynamic loads. Proceeding from the fact that the blade motion in stall flutter is characterized by torsion, as well as by bending in the plane of minimum rigidity while the in-plane deflections are usually small, the blade is considered to be elastic in torsion and bending flapwise and absolutely rigid chordwise.

The blade motion can be expressed by

$$\begin{cases} m\ddot{f} + [EIf'']'' - [Nf']' - m\sigma\ddot{\varphi} + \omega^2[m\sigma r\varphi]' = L_{aer} \\ I_m\ddot{\varphi} - [GT\varphi']' + \omega^2 I_m\varphi - m\sigma\ddot{f} - \omega^2 m\sigma r f' = M_{aer} \end{cases} \qquad (1)$$

with boundary conditions

$$\left.\begin{aligned} &f(0)=0 \\ &[EIf'']=0 \quad \text{or} \quad f'(0)=0 \\ &[GT\varphi']=C_{cont}\varphi_0+K_0\varphi_0 \end{aligned}\right\} \quad \text{with } r=0$$

$$\left.\begin{aligned} &[EIf'']'=0 \\ &[EIf'']=0 \\ &[GT\varphi']=0 \end{aligned}\right\} \quad \text{with } r=R$$

where

f = displacement of the blade elastic axis points relative to the plane of rotor rotation

φ = angle between the section inertia axis and the plane of rotor rotation

m = blade mass per unit length

I_m = blade moment of inertia per unit length relative to its flexural axis

EI = flexural blade rigidity

GT = torsional blade rigidity

σ = distance from the flexural axis of the blade to the centres of gravity of its sections

ω = rotor angular velocity

r = distance from the axis of rotation to the examined blade section

N = blade section centrifugal force $N=\omega^2\int_r^R mrdr$

The dots denote differentiation with respect to time; the primes, with respect to the blade radius.

The system of equations (1) is solved by using the Bubnov-Galerkin method; to do that, the modes and frequencies of natural flexural-torsional vibrations should be determined. The natural coupled flapwise flexural and torsional blade vibrations are usually described by the system of equations (1) in which the

right-hand side is equal to zero. To solve the system of these equations and find the natural flexural and torsional vibrations, the method given in Ref. 1 is used.

Besides the definition of the vibration modes, for constructing a model it is important to find the centres of the blade section turning, i.e. the points about which the sections turn with due account of elastic strain in the feathering hinge and static elastic blade twist.

The tail rotor induced speeds in hovering are computed by using the momentum theory, assuming at the same time that torsional blade vibrations in stall flutter have no influence on their value.

The tail rotor blade motion in stall flutter is found from a single flexural-torsional vibration mode. This approach is justified as the helicopter tail rotor tests have shown that the blade vibrations in stall flutter contain mainly a single harmonic component whose frequency is close to that of the natural flexural-torsional vibrations. The prediction of the blade motion in stall flutter from a single flexural-torsional vibration mode is additionally justified by the fact that the analysis of the resonance diagrams has shown no proximity to any vibration overtones whose interaction can serve as a basis for developing a self-oscillating model.

Using the Bubnov-Galerkin method equations (1) can be transformed into a differential equation with respect to the unknown time function $\delta(t)$

$$\ddot{\delta}+2n_0\varphi_0^2\dot{\delta}p+\delta p^2=\frac{1}{m^2}\int_0^R[M_{aer}\varphi(r)+L_{aer}f(r)]dr \qquad (2)$$

where

p = natural flexural-torsional blade vibration frequency

m = reduced mass of the blade oscillating in the considered mode

$2n_0$ = damping coefficient ratio

As the functions M and L are nonlinear and their dependence

is implicit, the equation is solved by numerical integration. The angular blade tip movement and initial velocity of motion are given as the initial conditions. The numerical integration method differs in that the expressions for unsteady aerodynamic loads Maer and L represent not only the nonlinear functions $\varphi, \dot{\varphi}$ and $\dot{f}_1$ but $\ddot{\varphi}$ and $\ddot{f}$ as well and, consequently $\ddot{\delta}$, thus equation (2) contains the unknown $\ddot{\delta}$ both in the explicit and implicit forms.

The algorithm for predicting the blade pitching moments is developed with due account of the dependence of the unsteady aerodynamic airfoil characteristics on Strouhal number and airfoil vibration frequencies.

Prediction of the unsteady aerodynamic forces and moments on the oscillating airfoil is the key factor in solving the stall flutter problem. The expressions for the oscillating airfoil force and moment given below have been taken from Ref. 2

$$L_y = 2\pi b \frac{\rho V}{2} c(k)\left[\varphi - \frac{\dot{y}}{U} - \left(a - \frac{1}{2}\right)\frac{b\dot{\varphi}}{2U}\right];$$
$$L_m = -\pi \frac{b^2}{4}\rho\left[\ddot{y} + a\frac{b}{2}\ddot{\varphi}\right]; \qquad (3)$$
$$L_h = \pi \frac{b^2}{4}\rho U^2 \frac{\dot{\varphi}}{U}; \qquad M_1 = -\frac{\pi}{128}\rho b^4 \ddot{\varphi};$$

Fig. 1 shows the points where the aerodynamic forces are applied.

The derived formulas allow to predict the force and moment on a thin airfoil oscillating relative to a small angle of attack in an ideal incompressible flow; they should be transformed to account for the thickness finiteness of the airfoil oscillating relative to a non-zero angle of attack in a real compressible flow. The airfoil unsteady aerodynamic characteristis $C_y(\alpha)$ and $C_m(\alpha)$ are characterized by the formation of hysteresis dependences and the phenomenon of stall delay in close proximity to the stall angle.

Stall delay and the formation of hysteresis dependences $C_y(\alpha)$ and $C_m(\alpha)$ of an oscillating airfoil have not been sufficiently highlighted in theoretical investigations. However, the

occurrence of stall flutter and thus the necessary search for means preventing it have demanded to develop semi-empirical prediction methods based on the available experimental data. A number of American authors have investigated the phenomenon of stall delay in their works trying to develop semi-empirical techniques for prediction of unsteady aerodynamic characteristics $C_y(\alpha)$ and $C_m(\alpha)$. Similar work has been done in the investigations devoted to the problem of tail rotor stall flutter.

Results of Analytical and Experimental Investigations Devoted to Tail Rotor Stall Flutter

Stall flutter has been found to occur on the blades of tail rotor designs of new types. It took place in hovering and, from a certain blade angle, it showed an abrupt growth of the variable component of the pitching moment whose frequency was not an integer multiple of the rotor speed. The frequency of different type rotors lay between 5/rev and 7/rev. The measured loads were several times higher than the ordinary level encountered in service, thus making the ensurance of strength and service lives of tail rotor designs and their control systems quite problematic.

The problem has turned out to be so grave that the fiberglass blades for the Mi-6 tail rotor were not put into production for this reason only.

In the course of developing the Mi-26 the tail rotor was supposed to be tested prior to its installation on the helicopter. With this object in view, a rig for testing tail rotors of heavy-lift helicopters was built; for this purpose a modified Mi-6 whose life had expired was used.The tested tail rotor was mounted on the main rotor shaft by means of an adapter; when rotating, it produced an upward thrust. The main gearbox of the helicopter had been modified to lower the gear ratio of the engine free turbine to the main rotor shaft to get a maximum rotor speed of 600 rpm which was higher than the nominal tail rotor speed. The

Mi-6 engines available in the rig produced a total power of 8.1 MW allowing to test the Mi-26 7.6 metre-diameter tail rotor over a wide range of blade angles at rotor speeds between 200 and 600 rpm. The maximum tail rotor speed exceeded the operating one by 10%, and the maximum blade angle exceeded the maximum value that could be implemented in operation by 17%. The blade bending and pitching moments under steady operating conditions were measured at constant values of the rotor speed and blade angle.

The tail rotor rig test results and the analysis made have allowed to find out the occurrence of stall flutter on the tail rotor blades. Fig. 2 shows a fragment of the oscillogram representing a record of the loads acting on the Mi-26 tail rotor blade at an operating rotor speed of 550 rpm and blade angle of 25 degrees. As can be seen from the record, the pitching moment varies mainly with a high frequency on which 1/rev is superimposed.The pitching moment variation frequency is 6.4/rev; in this case the blade vibration mode has a form typical of the 1st torsional mode. This has been found from the measurements of tangent stresses in several sections along the blade radius. Fig. 3 presents maximum amplitudes of the pitching moment vs blade angle obtained in the tests; it also shows a predicted dependence.

The rotor tests have allowed to establish another interesting phenomenon: the pitching moment amplitude reaches its maximum with the rotor speed and its dependence upon the latter is of resonance peak type (Fig. 4).

A search for means reducing the pitching moment amplitude value has shown that a change in the location of the centres of torsional rigidity of the blade sections can be quite effective. Fig. 5 shows the change in the pitching moment amplitude as the blade rigidity axis approaches the airfoil leading edge section. This result obtained analytically has been confirmed by the Mi-26

tail rotor tests. The blades were modified by incorporating airfoil shaped steel strips bonded to the spar outline. The strip running over 30% of the chord was bonded to the blade leading edge section along the blade span from r=0.4 to r=1.0. The strips have shifted the original location of the section rigidity centre line from 28% of the chord to 23.5-24%. The test results of this version have shown a much lower level of variable pitching moments as compared to that of the original version having no strips (Fig. 6).

Shifting the feathering hinge axis towards the blade leading edge section is also quite effective to reduce the pitching moment value in stall flutter. Fig. 7 presents the predicted pitching moment values for this case.

As part of the Mi-26 tail rotor development programme, the idea of shifting the centres of rigidity towards the leading edge section to reduce the pitching moment amplitudes has been implemented in the design of the blades for this helicopter.

REFERENCES

1. Mil' M.L et al. Helicopters. Calculation and Design.(Mil' M.L. i dr. Vertolety. Raschet i proyektirovaniye). Vol.2, 1967.
2. Nekrasov A.I. Airfoil Theory in Unsteady Flow. (Teorya kryla v nestatsionarnom potoke) Akad. Nauk SSSR, 1947

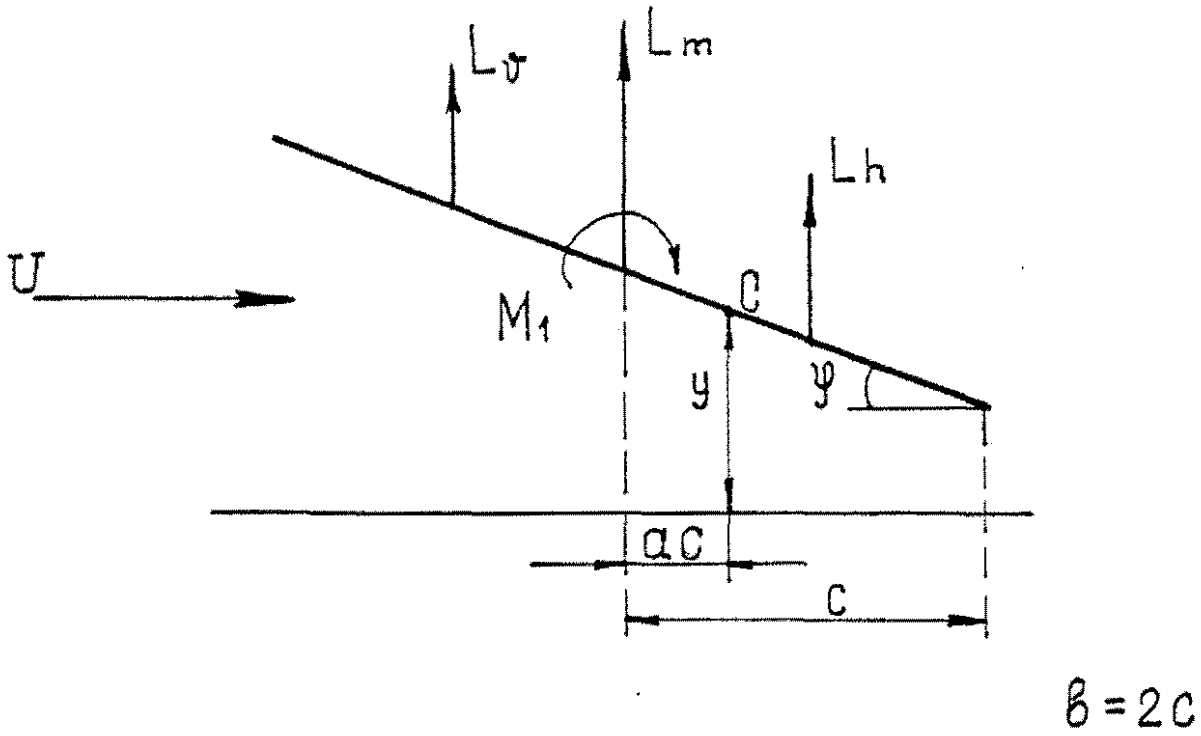

Fig. 1. Airfoil aerodynamic forces.

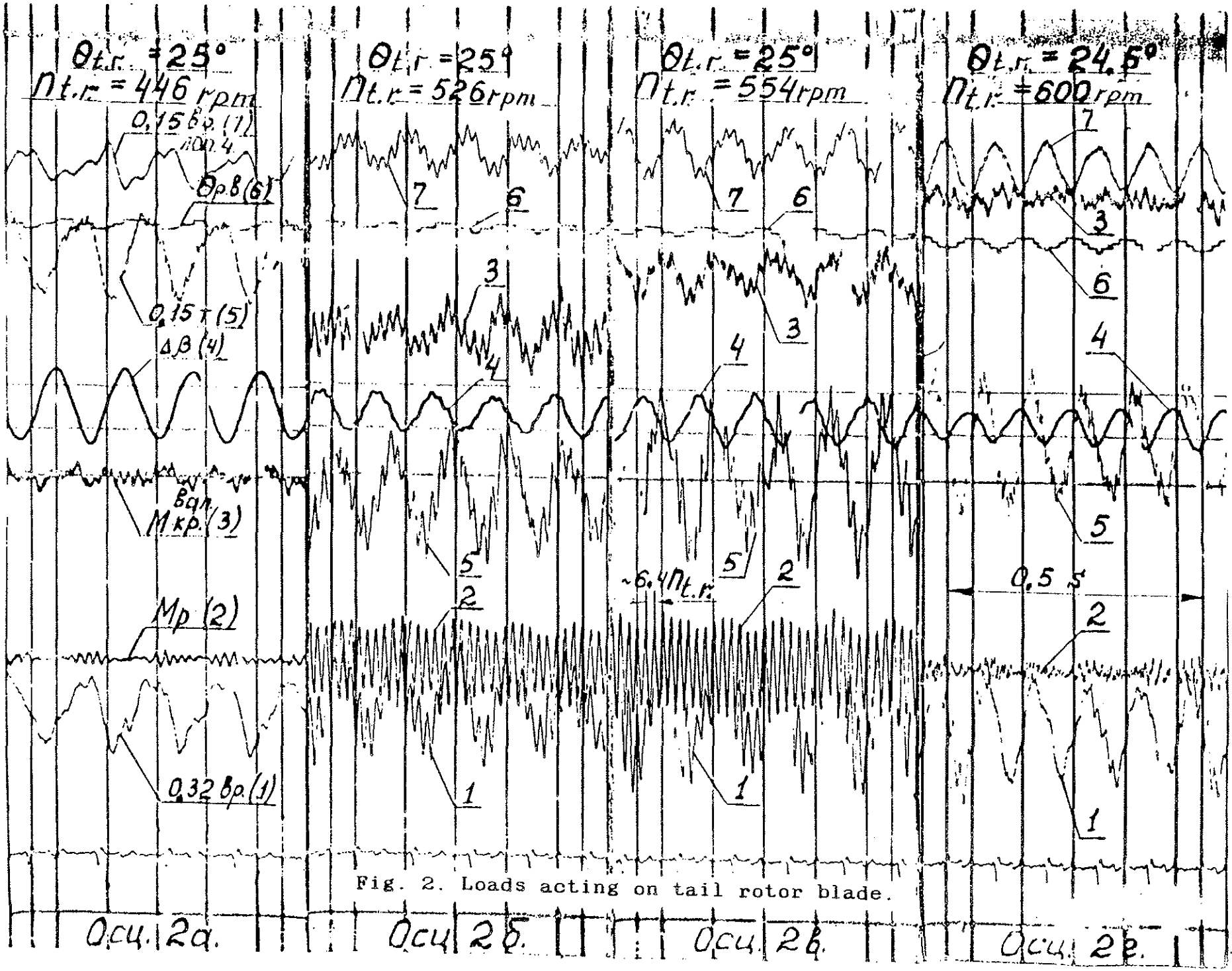

Fig. 2. Loads acting on tail rotor blade.

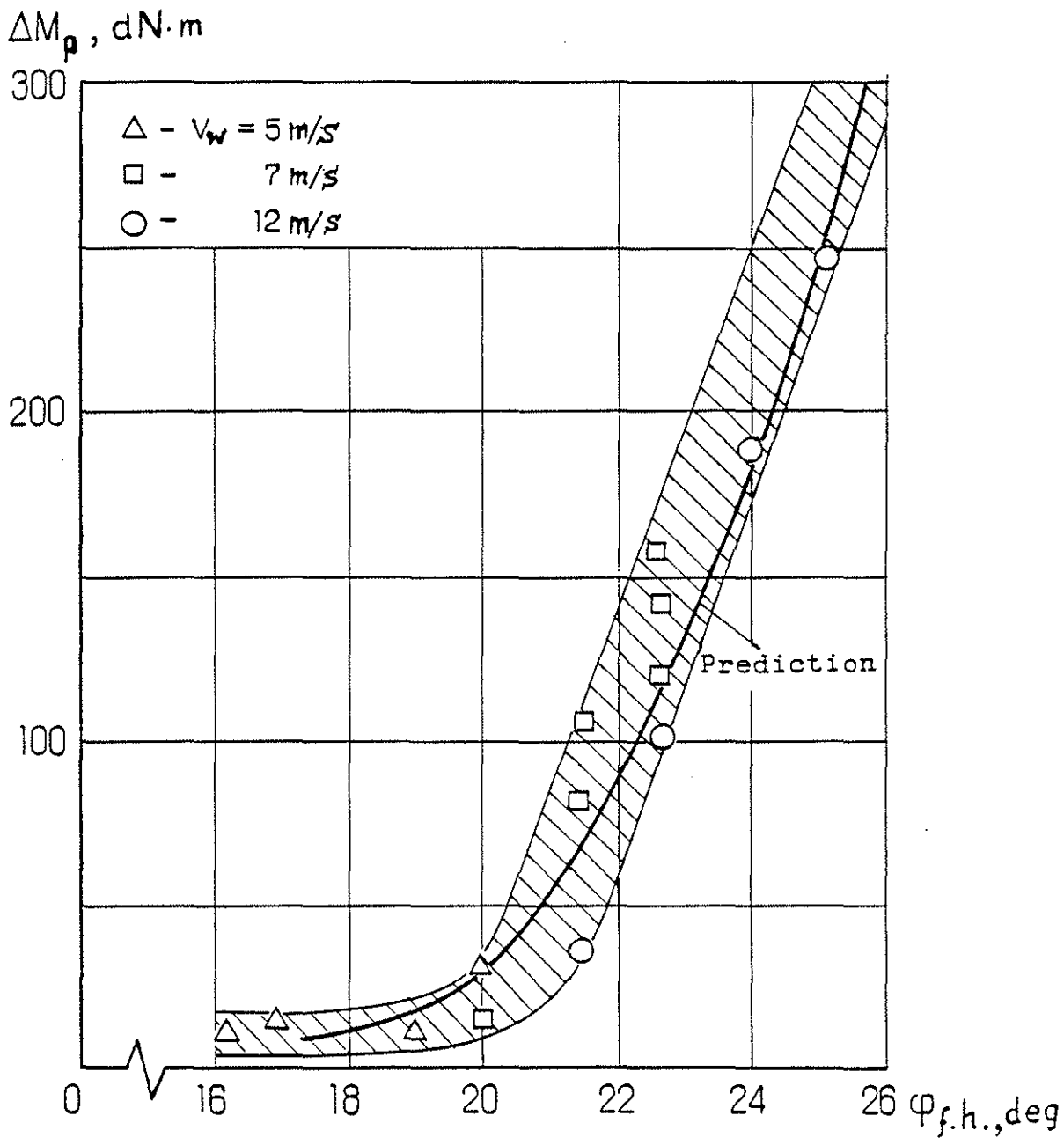

Fig. 3. Maximum pitching moment amplitudes vs blade angles.

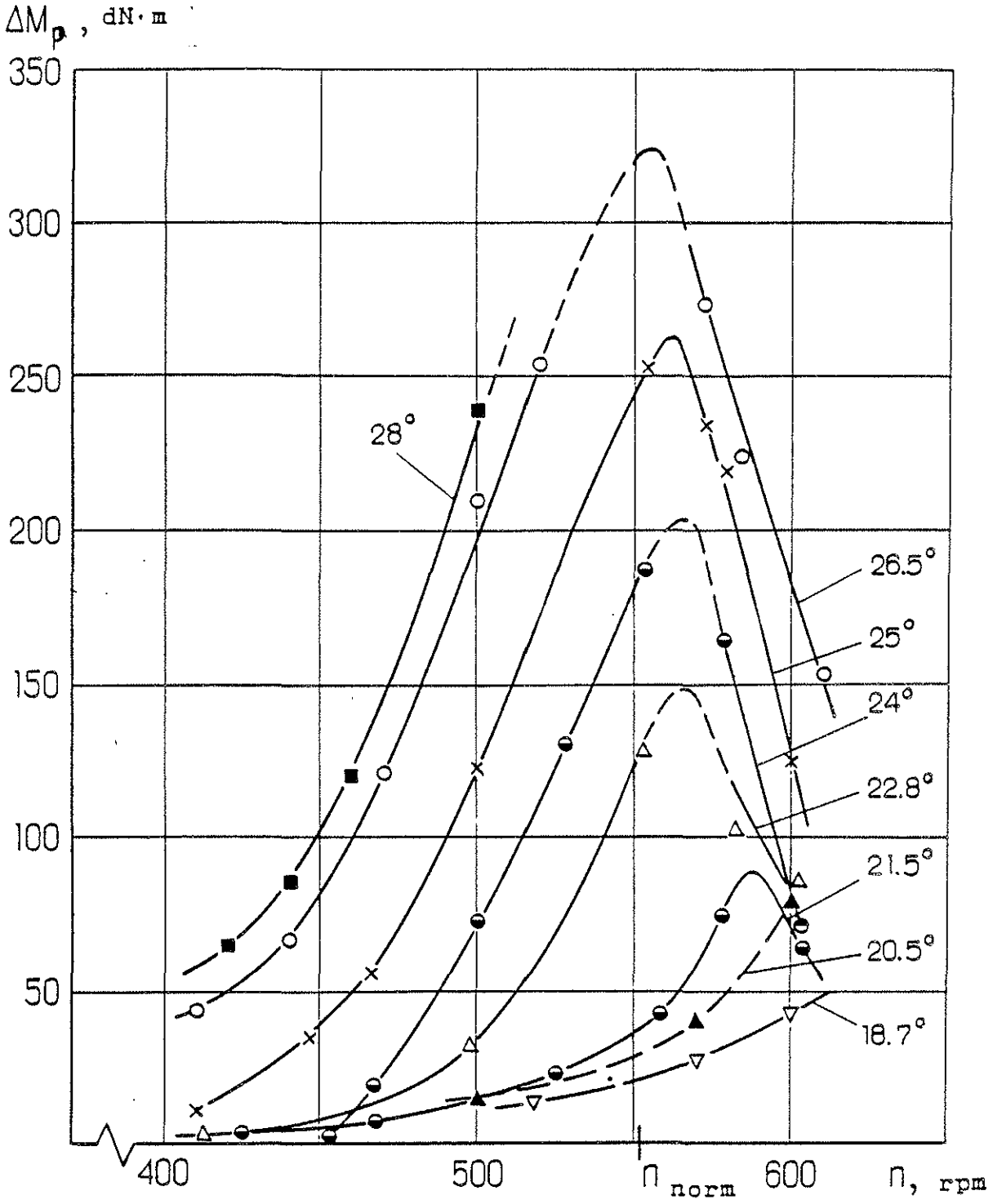

Fig. 4. Maximum pitching moment amplitudes vs rotor speed.

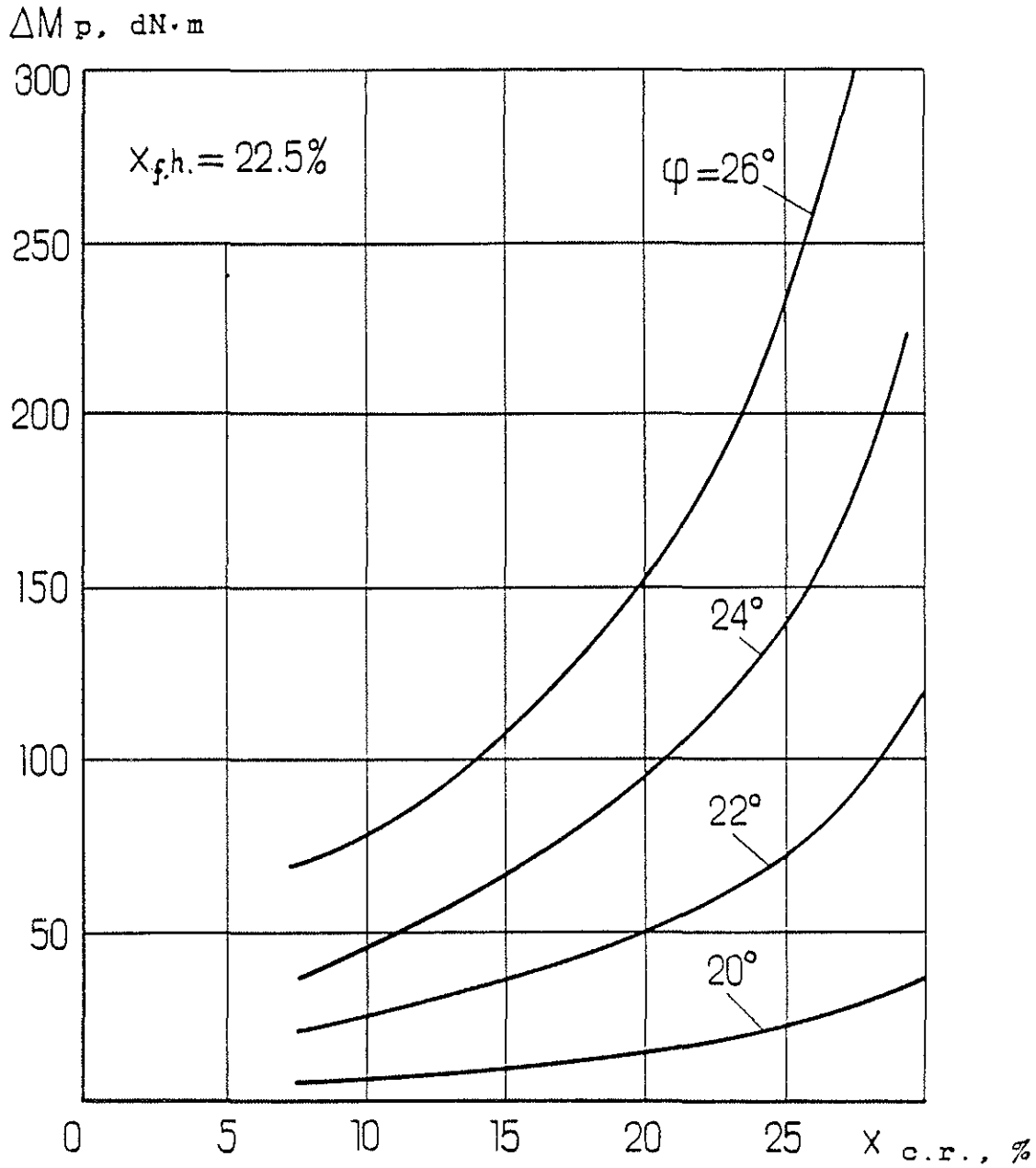

Fig. 5. Pitching moment amplitude of Mi-26 tail rotor blade vs flexural axis location.

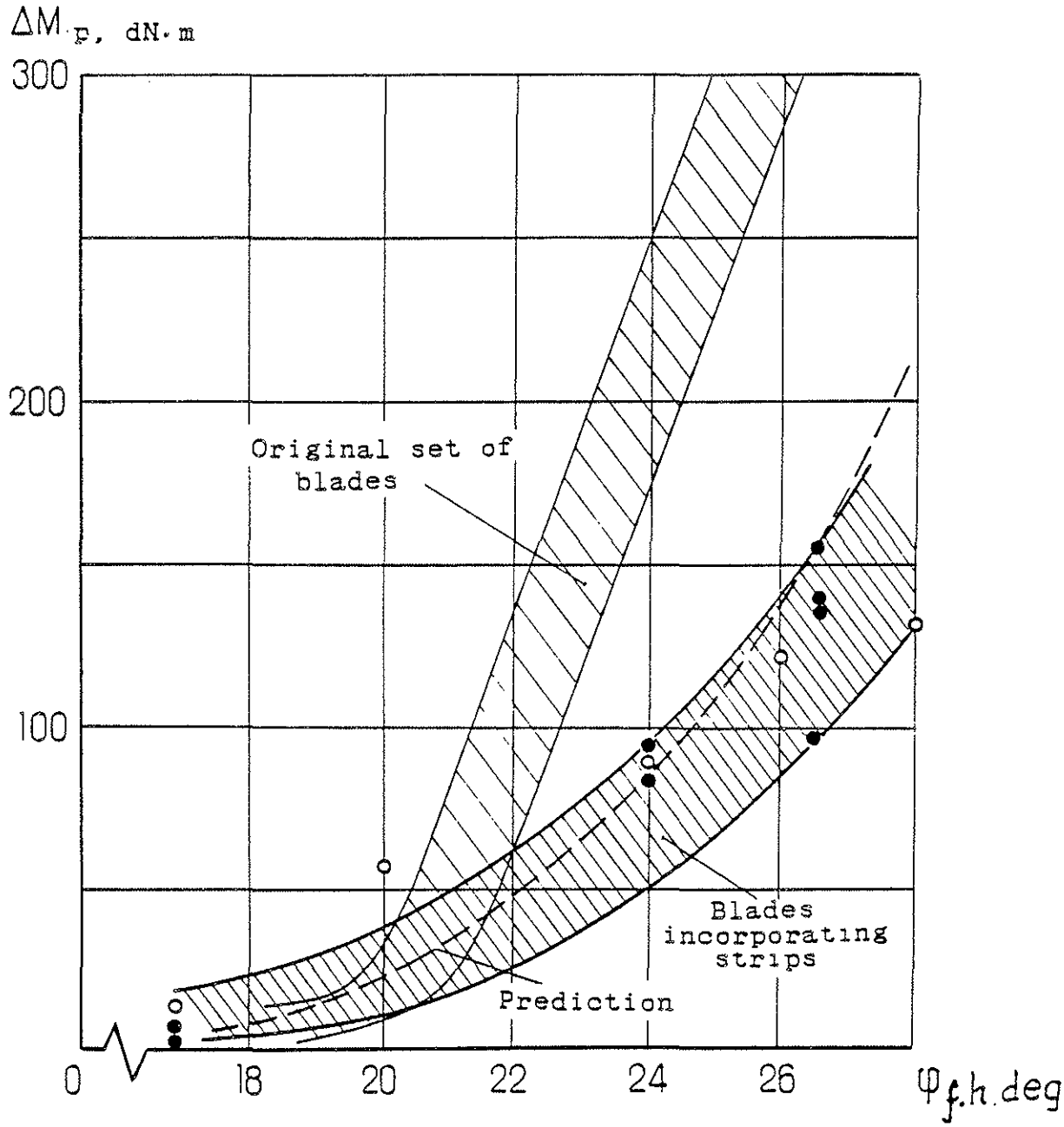

Fig. 6. Test results of tail rotor blades incorporating strips.

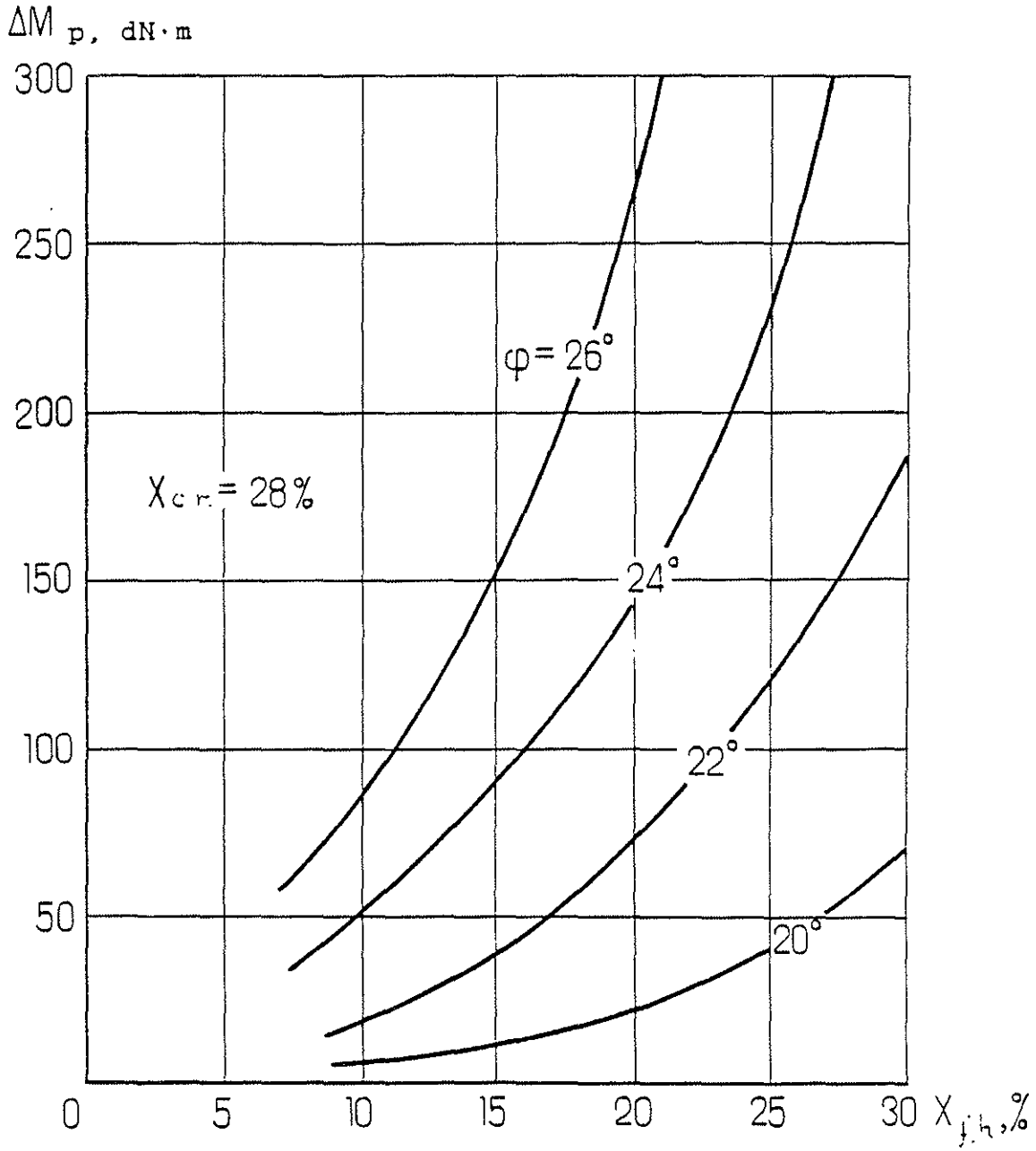

Fig. 7. Pitching moment amplitude vs feathering hinge location.